ARTICLE | Article in Press

FDG PET evidence suggests the left insula may be a hub for cognitive reserve in mild cognitive impairment

Rosa Liperoti · Maria Camilla Cipriani · Sonia Di Tella · Isabella Anzuino · Clio Scopetani Testa · Eleonora Clemente · Riccardo Calvani · Maria Rita Lo Monaco · Maria Lucia Calcagni · Fabrizio Cocciolillo · Maria Caterina Silveri

Received: 24 April 2025 / Accepted: 12 October 2026
© The Author(s) 2026

Abstract

Cognitive reserve (CR) refers to the ability to cope with the detrimental effects of ageing or brain pathology on cognition. Individuals with higher CR may maintain cognitive performance despite a greater burden of underlying brain pathology. This study aimed to characterize cerebral metabolic patterns associated with CR in subjects with amnestic mild cognitive impairment (aMCI) using [18]F-FDG PET/CT, and to identify brain regions associated with higher CR. Sixty-three subjects with aMCI were included in this cross-sectional study. Based on the Cognitive Reserve Index questionnaire (CRIq), 29 participants were classified as having high CR (HCR) and 34 as having low CR (LCR). Brain [18]F-FDG PET/CT scans were obtained in all participants and compared with those of 19 cognitively healthy subjects (HS). Voxel-wise analyses and volume-of-interest analyses were performed to assess regional metabolic differences, and multivariable regression models evaluated the association between CRIq and insular metabolism after adjustment for age and sex. Both HCR and LCR groups exhibited the characteristic temporo-parietal pattern of Alzheimer's disease-related hypometabolism compared with HS. Direct voxel-wise comparison between HCR and LCR identified a significant difference in the left anterior insula, where metabolism was relatively preserved in HCR. Left insular metabolism was positively associated with CRIq score independently of age and sex. These findings suggest that relatively preserved left insular metabolism is associated with higher CR in aMCI and identify the left anterior insula as a candidate neural substrate of CR. Future longitudinal studies will be important to confirm these findings and clarify the mechanisms possibly linking left insular metabolism to CR.

Introduction

The concept of cognitive reserve (CR) refers to the ability to cope with the detrimental effects of ageing and brain pathology on cognition[1]. CR results from genetic and environmental factors, with formal education being the most important determinant. The concept of CR was originally based on evidence showing that there is no direct correlation between the extent of neural damage and the severity of clinical symptoms[2]. This is consistent

This Article in Press is shared early to give you faster access to new research. It is citable and carries a permanent DOI. The final edited version will replace it automatically.



https://doi.org/10.1038/s41598-026-76261-x

Published online: 23 October 2026

scientific reports

with the extensive and long-standing evidence that the severity of neuropathological damage documented in post-mortem studies does not deterministically lead to dementia[3].

While some people experience a rapid decline in cognitive ability due to ageing or brain disease, others are more resilient to the effects of neural changes and maintain cognitive performance for longer. Higher educational attainment, particularly during early life, is considered one of the main proxies of CR and may contribute to delaying the clinical expression of cognitive impairment by allowing individuals to tolerate a greater burden of underlying brain pathology before cognitive symptoms become apparent[4]. Although CR is generally considered a protective factor acquired before the onset of brain changes leading to cognitive decline, increasing evidence suggests that it is not a fixed trait but can be modified throughout life by environmental exposures and life experiences[5]. This highlights the importance of maintaining cognitively and socially stimulating activities across the lifespan. Consistent with this concept, the literature indicates that higher CR is associated with a reduced risk of developing mild cognitive impairment (MCI)[6], dementia[7], and progression from MCI to dementia[8,9].

While the protective value of CR against cognitive impairment is well established, the neural mechanisms through which it is expressed and the substrates that support the maintenance of cognitive performance in the presence of ageing or brain pathology remain incompletely understood. One widely accepted framework proposes that CR is supported by brain reserve and neural compensation. Brain reserve refers to the structural characteristics of the brain including brain size, cortical thickness, neuronal and synaptic density, and the strength and architecture of neural connections, which together provide a substrate for resilience to pathology. Neural compensation, in contrast, refers to the brain's ability to recruit alternative neural networks or processing strategies in response to age- or disease-related changes[10]. Alongside these concepts, 'brain maintenance' refers to the relative preservation of brain structure and function through mechanisms of cellular repair and neuroplasticity, resulting in less age- or disease-related brain change than expected[11,12]. In this context, preserved synaptic integrity has been proposed as one of the strongest biological correlates of cognitive efficiency[13]. Together, CR, brain reserve, neural compensation, and brain maintenance contribute to the broader concept of 'brain resilience', defined as the brain's capacity to withstand the effects of ageing and neuropathology while maintaining cognitive function[12].

In neurodegenerative disorders, individuals with higher CR often exhibit a greater burden of brain pathology despite a comparable level of cognitive impairment, consistent with the concept that CR modulates the clinical expression rather than the development of disease[14,15]. Although this framework is widely accepted, the influence of CR on the subsequent clinical trajectory remains less clear. Recent evidence suggests that CR may delay the clinical expression of neurodegeneration during the early stages of disease, whereas its protective effect may diminish once clinical symptoms become established[16].

Functional neuroimaging, particularly [18]F-FDG PET, provides a valuable in vivo approach to investigate the relationship between CR and brain metabolism. Several studies have shown that individuals with higher CR may maintain cognitive performance despite lower cerebral metabolism, supporting the concept that CR modifies the relationship between pathology and clinical manifestations[17,18].

Nevertheless, the neural substrates through which CR is expressed remain poorly defined. Previous neuroimaging studies have implicated different regions and networks, including the hippocampus[18], posterior parietal and cingulate cortices[19], the left frontal cortex[9], and distributed temporal, parietal and limbic regions identified by structural MRI[20]. Together, these findings support the notion that resilience to Alzheimer's disease (AD) is likely to emerge from distributed large-scale brain networks rather than a single anatomical region. However, the evidence remains heterogeneous, and no consensus has yet emerged regarding the specific neural substrates underlying CR and resilience in neurodegenerative disease.

The aim of this study was to investigate cerebral metabolic patterns associated with CR in individuals with amnestic mild cognitive impairment (aMCI) using [18]F-FDG PET/CT and to identify potential candidate neural substrates of CR.

Methods

Participants

Study participants were selected from the ODINO (the DevelOpment of metabolic and functional markers of Dementia IN Older people) cohort. The ODINO study, described in detail previously[21], is a prospective cohort study including individuals who fulfilled the National Institute on Aging–Alzheimer's Association (NIA-AA) criteria for MCI[22]. Within this cohort, the diagnosis of amnestic MCI was established according to the Petersen criteria on the basis of clinical and comprehensive neuropsychological assessment[23]. The ODINO participants are seen annually at the Centre for Medicine of Ageing, Agostino Gemelli University Hospital IRCCS, Rome, since April 2020 for a total follow-up of three years or until conversion to dementia. Sociodemographic, clinical, laboratory, neuropsychological, neuroradiological and brain metabolic variables are available for individuals in the cohort.

A sample of individuals enrolled in the ODINO cohort between September 2022 and January 2024 was screened for the present cross-sectional study. Individuals with cerebrovascular disease, other neurological disorders, or less than five years of schooling were excluded. Sociodemographic, clinical and neuropsychological data were available for each subject. PET scans were performed within three months of the first clinical and neuropsychological assessment. Only subjects with an FDG-PET scan positive for an AD-related metabolic pattern and with complete Cognitive Reserve Index questionnaire (CRIq) data were included. FDG-PET positivity was defined qualitatively by the presence of the characteristic AD metabolic pattern, consisting of hypometabolism predominantly involving the temporo-parietal association cortex, with possible extension to the posterior cingulate cortex and precuneus, while relatively sparing the primary sensorimotor and primary visual cortices. The final sample included 63 aMCI subjects. The reporting of this cross-sectional study followed the Strengthening the Reporting of Observational Studies in Epidemiology (STROBE) guidelines[24].

CR assessment

All subjects completed the Cognitive Reserve Index questionnaire (CRIq) to assess CR[25]. The CRIq, a 20-item questionnaire, retrospectively collects information on cognitively stimulating activities since the age of 18, divided into education, work and leisure. It generates a total CRI score (CRIq_Tot) and three sub-indexes: CRI-Education (CRIq_Edu), based on years of education and training; CRI-Work Activity (CRIq_WA), reflecting cognitive engagement and responsibility in work roles (e.g. farmer, lawyer, professor); and CRI-Leisure Time (CRIq_LA), covering cognitively stimulating leisure activities (e.g. reading, sports, museum visits). CRIq scores can be classified into 5 ordered levels: low < 70; medium-low 70–84; medium 85–114; medium-high 115–130; high > 130. A CRIq score ≥ 115 was considered an index of high CR (HCR); a score ≤ 114 was considered an index of low CR (LCR). The mean CRIq is 100 ± 15.

Additional variables of interest

Participants' sociodemographic data were collected, including age, sex and level of education. Information on neurosensory deficits, family history of neurodegenerative or cardiovascular diseases, comorbidities and medications was also available. All participants underwent a comprehensive cognitive assessment including the Clinical Dementia Rating (CDR) scale and a battery of neuropsychological tests evaluating global cognitive function, verbal learning, episodic memory, verbal and visuospatial short-term memory, visuospatial abilities, language, attention, and executive function (see Supplementary Material, Table S1 for details). Functional status and level of independence were assessed using the Activities of Daily Living (ADL) and Instrumental Activities of Daily Living (IADL) scales. Physical performance was evaluated using the Short Physical Performance Battery (SPPB)

to further characterize the study population and assess the comparability of the HCR and LCR groups. Less than 1.0% of all included data regarding variables of interest were missing.

Image acquisition

Brain [18]F-FDG PET/CT scans were performed using a Biograph mCT64 PET/CT scanner (Siemens Healthineers) in 3D acquisition mode. Participants fasted for 6 h before radiotracer injection. PET acquisition began 40 min after an intravenous bolus of [18]F-FDG (3.7 MBq/kg) and lasted 20 min, with participants resting in a dimly lit, quiet room. Images were reconstructed using an iterative time-of-flight algorithm with CT-based attenuation corrections, all following identical technical parameters.

All PET examinations were performed at a single institution using identical acquisition and image reconstruction parameters, and a standardized imaging protocol derived from the procedural recommendations of the European Association of Nuclear Medicine and Molecular Imaging (EANM) for brain [18]F-FDG PET imaging. Participant preparation, fasting conditions, blood glucose assessment prior to tracer administration, injected activity, uptake time, acquisition protocol, and image reconstruction were standardized for all participants in order to minimize technical and physiological variability potentially affecting FDG uptake measurements. FDG-PET positivity was established by clinical visual interpretation. All PET scans were independently reviewed by two experienced nuclear medicine physicians, both blinded to the participants' CRIq classification and all study-specific variables. In cases of discordant interpretation, the final classification was established by consensus following joint image review.

After visual image analysis, voxel-wise comparisons were performed using Statistical Parametric Mapping version 8 (SPM8, Wellcome Department of Cognitive Neurology, London, UK). The SPM8 spatial normalisation algorithm aligned PET images to a dementia-specific [18]F-FDG template[26]. Each scan was checked for artefacts after normalisation. The output dimensions were: x = -90:91, y = -126:91, z = -72:109 (from the anterior commissure) with $2 \times 2 \times 2$ mm^3 isotropic voxels. Spatially normalized images were subsequently intensity normalized to correct for differences in total brain counts between scans using global mean scaling method by scaling the images to the average FDG uptake value in the whole brain. The use of proportional scaling was intended to reduce inter-subject variability related to global cerebral tracer uptake while allowing identification of regional metabolic differences associated with CR, Normalised images were smoothed with an isotropic Gaussian kernel of 8 mm FWHM. Group comparisons were performed using a two-sample t-test within the General Linear Model framework.

Statistical analysis was carried out through an unpaired 2-sample t-test with the Statistical Parametric Mapping (SPM). In order to provide an independent quantitative assessment of the regional metabolic differences identified by voxel-wise SPM analyses region masks were extracted from statistically significant clusters from the SPM comparison of the HCR and LCR groups using the MarsBaR toolbox (version 0.43)[27], which allows volume of interest (VOI) analysis within SPM and SUV (Standardized Uptake Values) were extracted for statistical comparison between groups.

Statistical analysis

Descriptive statistics were generated using means and standard deviations for continuous variables and proportions for categorical variables. The HCR and LCR groups were compared on key sociodemographic, clinical, functional and neuropsychological characteristics using unpaired two-sample t-test for continuous variables and chi-squared test for categorical variables. Descriptive statistics and group comparisons were performed using Jamovi statistical software (version 2.6.44).

Both groups were tested using a two-sample t-test for relative hypometabolism by comparison with a normal [18]F-FDG PET dataset consisting of 19 age-matched healthy subjects (HS).

A two-sample t-test was also performed to compare regional metabolic differences between groups. The resulting t-statistics were generated with a threshold of $p<0.005$. Only clusters with more than 120 voxels were considered significant. Given the exploratory nature of the study, statistical thresholds were defined a priori before data analysis. Statistical significance was set at an uncorrected voxel-level threshold of $p<0.005$, combined with a minimum cluster extent of 120 contiguous voxels. This analytical strategy was selected to balance statistical sensitivity and specificity in detecting biologically meaningful regional metabolic differences in an exploratory whole-brain analysis.

SUV values derived from both HS and study groups, were compared using ANOVA with Bonferroni correction ($p < 0.05$). As a complementary analysis, CR was examined as a continuous variable. To investigate the relationship between CR and regional cerebral glucose metabolism, linear regression analyses were performed using [18]F-FDG PET SUV value as the dependent variable and the CRIq total score as the independent variable. A first multivariable linear regression model was fitted including age and sex as covariates to assess whether the association between CRIq and glucose metabolism was independent of these potential confounders. To investigate whether sex modified the association between CR and cerebral metabolism, a second linear regression model including the interaction term between CRIq and sex (CRIq × sex) was fitted. Continuous variables were mean-centered before calculating the interaction term to reduce multicollinearity and facilitate interpretation of the regression coefficients. Regression coefficients (β), 95% confidence intervals (95% CI), coefficients of determination (R^2), and p-values were reported. Because of the relatively small sample size and the potential presence of heteroscedasticity, robust standard errors were estimated using the HC3 heteroscedasticity-consistent covariance estimator. Finally, correlation analyses were performed to investigate the association between left insular SUV values and neuropsychological performance across the study sample. All statistical tests were two-sided, and statistical significance was defined as $p < 0.05$.

Results

Of the study participants, 29 were included in the HCR group because they scored 115 or more on the CRIq, and 34 were included in the LCR group because they scored 114 or less on the same assessment. The main sociodemographic and clinical characteristics of the participants according to CR level are shown in Table 1. There were more women in the LCR group, where they made up over 60% of the group, compared with almost 40% in the HCR group. Years of education were on average higher in the HCR group than in the LCR group, as expected. All participants scored 0.5 on the CDR. The two study groups did not appear to differ in terms of neuropsychological performance, both in the assessment of global cognitive function and in the assessment of individual cognitive

Table 1 Socio-demographic and clinical characteristics of HCR and LCR groups.

Age, mean (SD)	HCR (*N*= 29)	LCR (*N*=34)	*p*-value
	76.55 (4.66)	75.77 (5.39)	0.542[#]
Female gender, n (%)	11 (37.90)	21 (61.80)	0.059[§]
Education, mean (SD)	13.93 (3.59)	9.03 (3.51)	**<0.001**[#]
ADL, mean (SD)	5.62 (0.49)	5.62 (0.49)	0.981[#]
IADL, mean (SD)	7.86 (0.44)	7.71 (0.76)	0.333[#]
SPPB, mean (SD)	9.97 (2.11)	9.59 (2.20)	0.493[#]
CDR, mean (SD)	0.50 (0.00)	0.50 (0.00)	1.000[#]
MMSE, mean (SD)	26.47 (2.90)	27.49 (1.91)	0.123[#]

ADL activities of daily living, *IADL* instrumental activities of daily living, *SPPB* short physical performance battery, *CDR* clinical dementia rating scale, *MMSE* mini-mental state examination (adjusted score for age and education according to normative data), *SD* standard deviation, *HCR* high cognitive reserve, *LCR* low cognitive reserve.

[#]Unpaired two sample t test.

[§]Chi-squared test. Significant p-value ($p<0.05$) are highlighted in bold font.

domains (see Supplementary Material -Table S1). No major differences were found between the two groups in terms of level of functional independence or physical performance, which was quite high in both groups, as indicated by the mean ADL, IADL and SPPB scores.

Voxel-wise analysis comparing HS and the whole sample of MCI subjects revealed reduced metabolism in the MCI group in the left temporo-parietal cortex (Fig. 1). Specifically, the cortical regions involved were the left inferior, middle and superior temporal gyrus, the superior and inferior parietal gyrus, the posterior cingulate cortex and the precuneus. The voxel-wise analysis between HS and the group of subjects with HCR showed reduced glucose metabolism distributed mainly in the left temporo-parietal regions (Fig. 2A), with a cluster of more severe hypometabolism localised mainly in the left middle temporal cortex (T-score 10.12) (see Table 2). The same voxel-wise analysis between HS and the group of subjects with LCR also revealed a predominantly left temporo-parietal glucose hypometabolism (Fig. 2B) of less pronounced magnitude than in subjects with HCR, with a T-score of 8.92 in the left middle temporal cortex (see Table 3).

In the direct comparison of the HCR and LCR groups, SPM analysis showed lower [18]F-FDG PET uptake in the left insula of subjects with LCR (Fig. 3). Specifically, the cluster of lower uptake was found in the left anterior insula long gyrus at -33/-20/15 mm (T-score 4.3)[28] of subjects with LCR compared to HCR.

To confirm the lower FDG uptake in the left insula of subjects with LCR, SUV values in the VOI of the left insula (see Fig. 4) were assessed. These were found to be reduced in both the HCR ($p=0.019$) and LCR (<0.001) groups compared to HS. In addition, SUV values were significantly lower in the left insula of subjects with LCR compared to subjects with HCR ($p<0.001$).

A multiple linear regression model was used to assess the association between CRIq total score and insular PET values while adjusting for age and sex. The overall model was significant ($N=63$, $R^2 = 0.188$, adjusted $R^2 = 0.147$, robust model $p=0.006$). Higher CRIq scores remained independently associated with higher insular values (B = 0.0117 per CRIq point, 95% CI 0.0019–0.0216, $p=0.020$), whereas age was not significantly associated with insular values ($p=0.878$). Sex showed a borderline, but non-significant, association ($p=0.058$). A second model including the CRIq-by-sex interaction did not identify a significant interaction effect (B = −0.0058, 95%

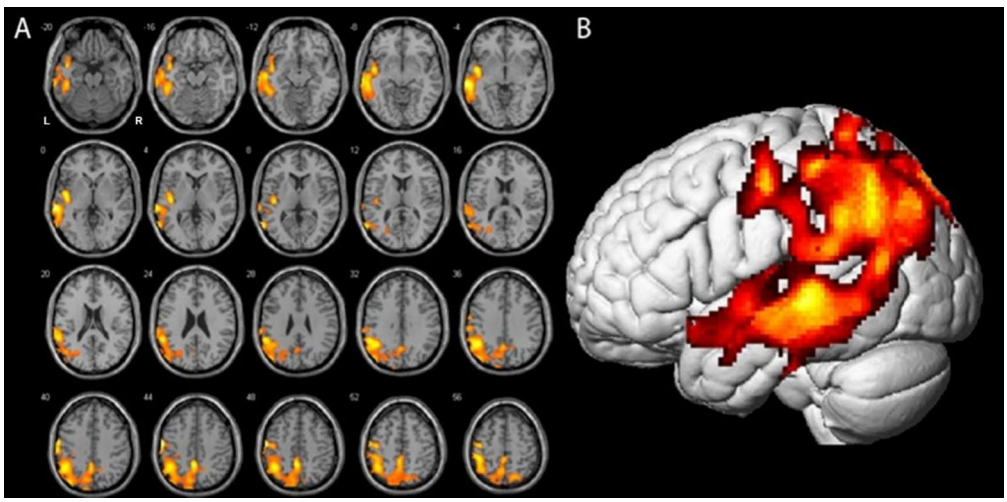


Fig. 1 Axial slices (**A**) and three-dimensional brain surface rendering (B) illustrating the results of the whole-brain SPM analysis. Colour-coded regions represent brain areas showing significantly reduced [18]F-FDG uptake in the overall Mild Cognitive Impairment (MCI) cohort compared with Healthy Subjects (HS). Statistical maps are displayed at a voxel-level threshold of $p < 0.005$ (uncorrected) with a cluster extent threshold of $k > 120$ contiguous voxels. Abbreviations: SPM, Statistical Parametric Mapping; MCI, Mild Cognitive Impairment; HS, Healthy Subjects.

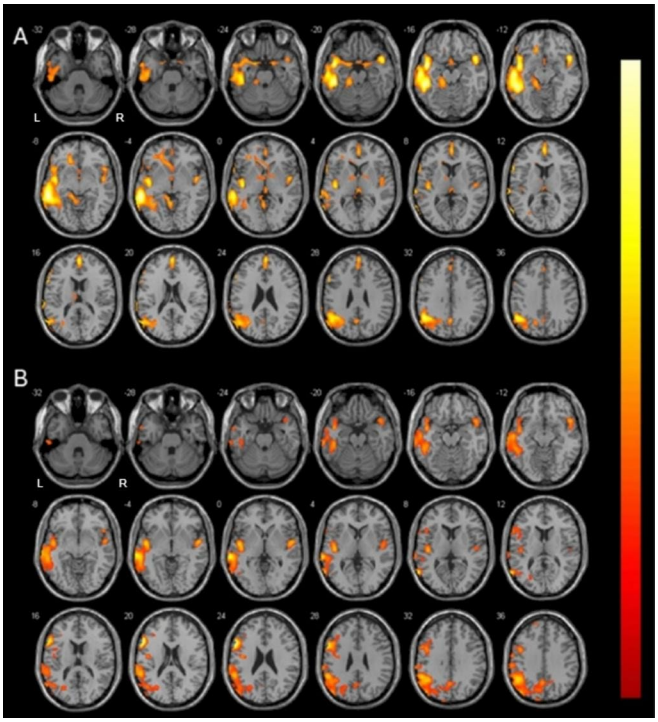


Fig. 2 Axial slices showing the results of the whole-brain SPM analyses comparing High Cognitive Reserve (HCR) (**A**) and Low Cognitive Reserve (LCR) (**B**) patients with Healthy Subjects (HS). Colour-coded regions indicate brain areas showing significantly reduced [18]F-FDG uptake relative to HS. Statistical maps are displayed at a voxel-level threshold of $p < 0.005$ (uncorrected) with a cluster extent threshold of k > 120 contiguous voxels. Although these maps do not represent a statistically significant direct comparison between the HCR and LCR groups, both analyses demonstrate a predominant pattern of left temporo-parietal hypometabolism relative to healthy subjects. Qualitatively, the spatial extent of hypometabolism appears less pronunced in the LCR group than in the HCR group. Abbreviations: SPM, Statistical Parametric Mapping; HCR, High Cognitive Reserve; LCR, Low Cognitive Reserve; HS, Healthy Subjects.

Table 2 Whole brain statistics from SPM analysis of the group of subjects with HCR.

SPM results showing the clusters (brain areas) where brain glucose metabolism was significantly hypometabolic compared with HS. MNI stereotactic coordinate for center voxel (x, y,z), the T scores and Z equivalent scores.

SPM statistical parametric mapping, *HCR* high cognitive reserve, *HS* healthy subjects, *MNI* Montreal Neurological Institute, *L* left, *R* right.

T	Z equivalent	x, y,z {mm}	x, y,z {mm}	x, y,z {mm}	Labels
10.12	7.30	-60	-36	-6	Temporal_Mid_L
9.98	7.24	-46	2	-18	Temporal_Pole_L
9.73	7.13	-52	-40	-14	Temporal_Mid_L
8.05	6.32	50	14	-14	Temporal_Pole_Sup_R
7.12	5.81	0	56	16	Frontal_Sup_Medial_L
5.79	4.99	-16	32	-10	Frontal_Sup_Orb_L
5.75	4.96	-48	-8	-2	Insula_L
5.72	4.93	-16	-32	-18	Fusiform_L
5.47	4.77	-14	-36	-10	ParaHippocampal_L
5.45	4.76	-6	26	-2	Cingulum_Ant_L
5.43	4.75	-2	-62	30	Precuneus_L
5.42	4.74	0	-48	40	Precuneus_L
5.14	4.54	-32	40	-2	Frontal_Mid_L
4.90	4.37	2	-44	54	Precuneus_R
4.82	4.31	46	-16	6	Heschel_R
3.78	3.50	2	30	44	Frontal_Sup_Medial_L

CI −0.0274–0.0159, $p = 0.601$), indicating that the association between CRIq and insular values did not significantly differ according to sex.

As a complementary analysis, CR was examined as a continuous variable. Linear regression demonstrated a significant positive association between total CRIq score and left insular SUV (unstandardized B = 0.0147, 95% CI 0.0051–0.0244; standardized $\beta = 0.363$; $p = 0.003$; $R^2 = 0.132$).

Finally, we tested the association between left-insular SUV and cognitive performance across the sample and found no significant positive associations (e.g. MMSE $\rho = -0.15$, $p = 0.27$; Rey immediate recall showed a weak negative trend, $\rho = -0.25$, $p = 0.05$; Rey delayed recall $\rho = -0.04$, $p = 0.74$; semantic fluency $\rho = -0.13$, $p = 0.32$).

Table 3 Whole brain statistics from SPM analysis of subjects with LCR.

T	Z equivalent	x, y,z {mm}	x, y,z {mm}	x, y,z {mm}	Labels
8.92	6.89	-64	-62	8	Temporal_Mid_L
8.59	6.72	-55	-23	46	Parietal_Inf_L
8.37	6.61	-66	-32	0	Temporal_Mid_L
8.28	6.56	28	-38	72	Postcentral_R
7.80	6.30	26	-20	76	Precentral_R
6.97	5.81	-41	-7	-2	Insula_L
6.43	5.47	52	16	-12	Temporal_Pole_Sup_R
6.29	5.38	2	26	62	Frontal_Sup_Medial_L
6.23	5.34	-30	58	18	Frontal_Mid_L
5.97	5.17	-4	-60	39	Precuneus_L
5.88	5.11	52	-32	64	Postcentral_R
5.75	5.02	-7	-57	36	Precuneus_L
5.34	4.73	-28	62	2	Frontal_Mid_L
4.67	4.24	8	36	60	Frontal_Sup_Medial_R
4.51	4.11	-2	22	48	Supp_Motor_Area_L

SPM results showing the clusters (brain areas) where brain glucose metabolism was significantly hypometabolic compared with HS. MNI stereotactic coordinate for center voxel (x, y,z), the T scores and Z equivalent scores.

SPM statistical parametric mapping, *LCR* low cognitive reserve, *HS* healthy subjects, *MNI* Montreal Neurological Institute, *L* left, *R* right.

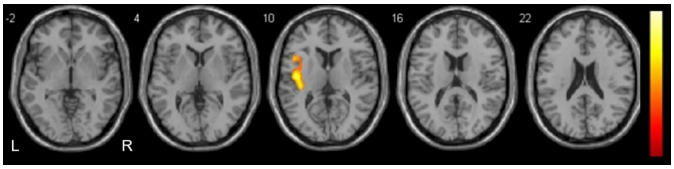


Fig. 3 Axial magnetic resonance slices showing the results of the direct whole-brain SPM comparison between High Cognitive Reserve (HCR) and Low Cognitive Reserve (LCR) patients. The colour-coded cluster identifies the left insular cortex, the only brain region showing a statistically significant difference in [18]F-FDG uptake between the two groups. Patients with LCR exhibited significantly lower glucose metabolism in the left insula compared with patients with HCR. Statistical maps are displayed at a voxel-level threshold of $p < 0.005$ (uncorrected) with a cluster extent threshold of $k > 120$ contiguous voxels. *SPM* statistical parametric mapping, *HCR* high cognitive reserve, *LCR* low cognitive reserve.

Discussion

The present study investigated the relationship between CR and cerebral glucose metabolism in individuals with aMCI, with the aim of identifying brain regions potentially associated with the neural substrates of CR. The principal finding was that, despite comparable cognitive and functional performance, participants with higher CR exhibited relatively preserved metabolism in the left anterior insula.

Consistent with previous FDG-PET studies[14,15,18], both HCR and LCR groups showed the characteristic AD-related pattern of left temporoparietal hypometabolism compared with healthy subjects. Although the statistical maps suggested a qualitatively more extensive pattern of hypometabolism in participants with HCR, direct voxel-wise comparison between the two groups identified a significant difference only in the left anterior insula. This observation was further supported by the VOI analysis, which demonstrated reduced left insular SUV in both HCR and LCR groups relative to healthy subjects, with significantly lower values in participants with LCR. Moreover, the positive association between CRIq score and left insular SUV remained significant after adjustment for age and sex, and was further confirmed when CR was analysed as a continuous variable.

The present findings are also consistent with previous neuroimaging evidence suggesting that the left anterior insula may contribute to mechanisms of neural resilience in the early stages of AD. In a resting-state fMRI study higher and more extensive brain activity was documented in the left insula, left inferior frontal gyrus and right precentral gyrus in healthy ApoE ε4 allele carriers compared to healthy ApoE ε4 allele non-carriers and MCI individuals[29]. The authors interpreted this pattern as a possible expression of resistance to AD pathology, within the framework of the Scaffolding Theory of Aging and Cognition (STAC)[30]. According to STAC, the progressive

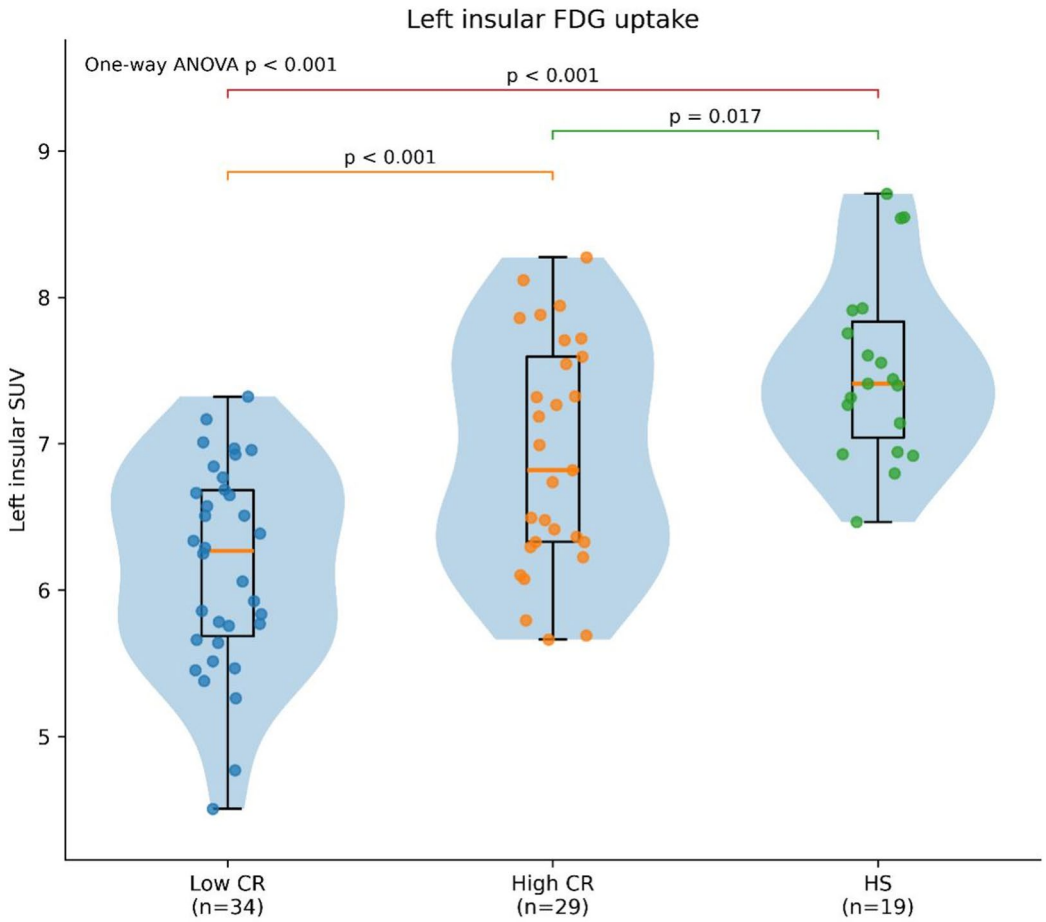


Fig. 4 Distribution of left insular glucose uptake according to cognitive reserve. Violin plots show the distribution of absolute standardized uptake values measured in the left insular volume of interest in participants with low cognitive reserve (Low CR), high cognitive reserve (High CR), and healthy subjects (HS). Individual points represent single participants. The internal box indicates the interquartile range, the horizontal line indicates the median, and the whiskers extend to values within 1.5 times the interquartile range. Between-group differences were assessed using one-way analysis of variance followed by Tukey's post-hoc test.

recruitment of anterior brain regions represents a lifelong adaptive response that helps maintain cognitive performance despite age-related reductions in neural efficiency. Similar to the concept of CR, STAC proposes that this 'compensatory scaffolding' is shaped by environmental stimuli, primarily education. Although these adaptive mechanisms may eventually become insufficient as neurodegeneration progresses[30], functional neuroimaging studies suggest that, during the preclinical and early clinical stages of AD, increased recruitment of anterior brain regions may contribute to maintaining cognitive performance despite the presence of underlying pathology[31].

The left anterior insula, through its dense reciprocal connections with frontal cortical regions[32], may represent one of the anterior structures involved in the adaptive recruitment proposed by the STAC model. Beyond this framework, however, the functional organization of the insula also provides a broader network-based perspective for interpreting our findings[33]. The anterior insula is widely recognized as a major hub of the Salience Network, where it plays a pivotal role in coordinating interactions among large-scale brain networks[34]. In addition to its established involvement in emotional, affective, social, and interoceptive processing, the anterior insula contributes to higher-order attentional and executive control. By detecting salient environmental stimuli, it facilitates the dynamic switching between the Default Mode Network (deactivated) and the Central Executive Network (activated) during cognitively demanding tasks[35], and thus promotes the access of stimuli to attentional systems

and working memory for further processing. From this perspective, the extensive connectivity of the anterior insula and its central role in integrating information across distributed neural systems provide a biologically plausible framework for interpreting the present findings. Indeed, the relatively preserved metabolism of the left anterior insula observed in participants with higher CR may reflect the preservation of a key network hub involved in maintaining efficient communication across large-scale brain systems. Consistent with this interpretation, previous neuroimaging studies have suggested relative resistance of the Salience Network to AD pathology[29,36,37]. Accordingly, the relatively preserved metabolism of the left anterior insula in individuals with higher CR may reflect the maintenance of network integrity developed through lifelong environmental enrichment and cognitive stimulation. However, this interpretation remains speculative and requires confirmation in longitudinal studies specifically designed to investigate the neural mechanisms linking CR, brain networks, and resilience to neurodegeneration.

The left-sided localization of our findings was unexpected. One possible explanation is that the association between CR and the left anterior insula may relate to cognitive processes that are predominantly lateralized to the left hemisphere, including language. This hypothesis is indirectly supported by the observation that education, one of the principal proxies of CR, is fundamentally language-based, and by evidence suggesting that bilingualism may contribute to CR and resilience to neurodegenerative disease[38]. However, the present findings are exploratory and do not demonstrate a specific role of language or left hemispheric specialization in the mechanisms underlying CR. Rather, they provide a rationale for future studies specifically designed to investigate whether language-related networks contribute to the neural substrates of CR.

An alternative interpretation of our findings should also be considered. Individuals with higher CR may reach the clinical threshold for MCI at a more advanced stage of the underlying neuropathological process. Therefore, the relatively preserved metabolism of the left insula may not necessarily reflect active compensatory recruitment but could also be related to differences in regional disease progression or premorbid neural efficiency. Nevertheless, it is noteworthy that all participants were evaluated at the same clinical stage of disease (CDR = 0.5) and that the HCR and LCR groups showed comparable cognitive, functional (ADL, IADL), and physical (SPPB) performance. Furthermore, although both groups exhibited the characteristic temporoparietal pattern of AD-related hypometabolism, direct voxel-wise comparison identified a significant between-group difference only in the left anterior insula. This observation supports the hypothesis that preserved left insular metabolism may be specifically associated with higher CR. However, given the cross-sectional design and the exploratory nature of the present study, our findings should be regarded as hypothesis generating and require confirmation in larger longitudinal cohorts.

Several limitations of the present study should be acknowledged. First, the cross-sectional design did not allow the assessment of the temporal relationship between cerebral metabolism, CR, and clinical progression. Consequently, our findings do not allow conclusions regarding the mechanisms linking preserved left insular metabolism to CR. Second, the relatively small sample size, together with the limited number of healthy controls, may have reduced the statistical power of the analyses. Furthermore, neuropsychological data were not available for the healthy control group, precluding direct comparisons of cognitive performance between MCI and healthy subjects. Another limitation concerns the absence of AD-specific biological biomarkers and APOE genotyping. Although the clinical, neuropsychological, and FDG-PET findings were consistent with the AD continuum, biological confirmation of the underlying pathology was not available. In addition, the voxel-wise analyses were performed using an exploratory statistical threshold without whole-brain correction for multiple comparisons. Although this approach has been widely adopted in exploratory neuroimaging studies, the present findings should be interpreted cautiously until replicated in larger independent cohorts. Finally, the study findings derive from a single cohort and may not be generalizable to subjects with MCI from different clinical settings or geographical populations.

In conclusion, our findings provide further evidence that individuals with aMCI exhibit the characteristic temporoparietal pattern of cerebral hypometabolism. Within this context, relatively preserved metabolism of the left anterior insula was associated with higher CR and represented the only significant metabolic difference identified

between participants with high and low CR. Although the cross-sectional design precludes conclusions regarding the underlying mechanisms, these findings suggest that the left anterior insula may represent a candidate neural substrate associated with CR. Future longitudinal studies in larger, independent cohorts incorporating disease-specific biomarkers will be essential to confirm these findings and to clarify the neural mechanisms linking preserved left insular metabolism to CR.

Supplementary Information The online version contains supplementary material available at https://doi.org/10.1038/s41598-026-76261-x.

Author contributions R.L., M.C.C., M.C.S. and M.R.L.M. contributed to the study concept, design and conduction, manuscript writing and study coordination; I.A., S.D.T., C.S.T., E.C. and R.C. contributed to data collection, analysis and interpretation; M.L.C. and F.C. contributed to PET scan acquisition and data analysis.

Funding The study received funding from 'progetto PRIN 2022 Brain plasticity in ageing and pathology', Prot. 2022H2J3N3 - CUP J53D23008030008; National Recovery and Resilience Plan, Investment PE8 - Project Age-It: "Ageing Well in an Ageing Society"/Next Generation EU. Funding sources had no role in the study design, in data collection, analysis and interpretation, in the writing of the paper and in the decision to submit the paper for publication.

Data availability The datasets generated and analysed during the current study contain sensitive clinical information and cannot be made publicly available or directly shared because of ethical, privacy, and institutional restrictions. Upon reasonable request to the corresponding author, controlled read-only access to the relevant data files may be considered for scientific verification purposes, subject to approval by the relevant Ethics Committee and in accordance with applicable institutional data-access and data-protection policies.

Declarations

Competing interests The authors declare no competing interests.

Ethical approval and informed consent The study was approved by the Ethics Committee of the Catholic University of the Sacred Heart, Rome (Protocol No. 230/19). Written informed consent was obtained from all participants prior to enrolment in accordance with the Declaration of Helsinki and the approved study protocol.

Open Access This article is licensed under a Creative Commons Attribution-NonCommercial-NoDerivatives 4.0 International License, which permits any non-commercial use, sharing, distribution and reproduction in any medium or format, as long as you give appropriate credit to the original author(s) and the source, provide a link to the Creative Commons licence, and indicate if you modified the licensed material. You do not have permission under this licence to share adapted material derived from this article or parts of it. The images or other third party material in this article are included in the article's Creative Commons licence, unless indicated otherwise in a credit line to the material. If material is not included in the article's Creative Commons licence and your intended use is not permitted by statutory regulation or exceeds the permitted use, you will need to obtain permission directly from the copyright holder. To view a copy of this licence, visit http://creativecommons.org/licenses/by-nc-nd/4.0/.

References

1. Stern, Y. Cognitive reserve in ageing and Alzheimer's disease. *Lancet Neurol.* **11**, 1006–1012 (2012).
2. Blessed, G., Tomlinson, B. E. & Roth, M. The Association Between Quantitative Measures of Dementia and of Senile Change in the Cerebral Grey Matter of Elderly Subjects. *Br. J. Psychiatry*. **114**, 797–811 (1968).
3. Powell, A., Chan, K., Shepherd, C. E. & Brodaty, H. Cognitive resilience in ageing: determinants and interventions. *Lancet Neurol.* **25**, 492–505 (2026).
4. Lövdén, M., Fratiglioni, L., Glymour, M. M., Lindenberger, U. & Tucker-Drob, E. M. Education and Cognitive Functioning Across the Life Span. *Psychol. Sci. Public. Interest.* **21**, 6–41 (2020).
5. Kremen, W. S. et al. Cognitive Reserve and Related Constructs: A Unified Framework Across Cognitive and Brain Dimensions of Aging. *Front. Aging Neurosci.* **14**, 834765 (2022).
6. Corbo, I., Marselli, G., Di Ciero, V. & Casagrande, M. The Protective Role of Cognitive Reserve in Mild Cognitive Impairment: A Systematic Review. *JCM* **12**, 1759 (2023).

7. Nelson, M. E., Jester, D. J., Petkus, A. J. & Andel, R. Cognitive Reserve, Alzheimer's Neuropathology, and Risk of Dementia: A Systematic Review and Meta-Analysis. *Neuropsychol. Rev.* **31**, 233–250 (2021).
8. Iraniparast, M. et al. Cognitive reserve and mild cognitive impairment: Predictors and rates of reversion to intact cognition vs progression to dementia. *Neurology* **98** (2022).
9. Franzmeier, N. et al. Cognitive reserve moderates the association between functional network anti-correlations and memory in MCI. *Neurobiol. Aging*. **50**, 152–162 (2017).
10. Pappalettera, C., Carrarini, C., Miraglia, F., Vecchio, F. & Rossini, P. M. Cognitive resilience/reserve: Myth or reality? A review of definitions and measurement methods. *Alzheimer's Dement.* **20**, 3567–3586 (2024).
11. Cabeza, R. et al. Maintenance, reserve and compensation: the cognitive neuroscience of healthy ageing. *Nat. Rev. Neurosci.* **19**, 701–710 (2018).
12. Stern, Y. et al. A framework for concepts of reserve and resilience in aging. *Neurobiol. Aging*. **124**, 100–103 (2023).
13. Taddei, R. N. & Duff, K. E. Synapse vulnerability and resilience across the clinical spectrum of dementias. *Nat. Rev. Neurol.* **21**, 353–369 (2025).
14. Garibotto, V. et al. Education and occupation as proxies for reserve in aMCI converters and AD: FDG-PET evidence. *Neurology* **71**, 1342–1349 (2008).
15. Kemppainen, N. M. et al. Cognitive reserve hypothesis: Pittsburgh Compound B and fluorodeoxyglucose positron emission tomography in relation to education in mild Alzheimer's disease. *Ann. Neurol.* **63**, 112–118 (2008).
16. Guo, L., Zhou, Y., Lu, H. & Fung, H. H. The moderating effect of cognitive reserve on the association between neuroimaging biomarkers and cognition: A systematic review. *Neurobiol. Aging*. **156**, 10–29 (2025).
17. Ewers, M., Insel, P. S., Stern, Y. & Weiner, M. W. For the Alzheimer's Disease Neuroimaging Initiative (ADNI). Cognitive reserve associated with FDG-PET in preclinical Alzheimer disease. *Neurology* **80**, 1194–1201 (2013).
18. Kato, T. et al. Effect of cognitive reserve on amnestic mild cognitive impairment due to Alzheimer's disease defined by fluorodeoxyglucose-positron emission tomography. *Front. Aging Neurosci.* **14**, 932906 (2022).
19. Bauckneht, M. et al. Metabolic correlates of reserve and resilience in MCI due to Alzheimer's Disease (AD). *Alz Res. Therapy*. **10**, 35 (2018).
20. Williams, M. E. et al. Neuroimaging Predictors of Cognitive Resilience against Alzheimer's Disease Pathology. *Ann. Neurol.* **97**, 1038–1050 (2025).
21. Picca, A. et al. The develOpment of metabolic and functional markers of Dementia IN Older people (ODINO) Study: Rationale, Design and Methods. *JPM* **10**, 22 (2020).
22. Albert, M. S. et al. The diagnosis of mild cognitive impairment due to Alzheimer's disease: Recommendations from the National Institute on Aging-Alzheimer's Association workgroups on diagnostic guidelines for Alzheimer's disease. *Alzheimer's Dement.* **7**, 270–279 (2011).
23. Petersen, R. C. et al. Mild cognitive impairment: a concept in evolution. *J. Intern. Med.* **275**, 214–228 (2014).
24. Von Elm, E. et al. The Strengthening the Reporting of Observational Studies in Epidemiology (STROBE) statement: guidelines for reporting observational studies. *J. Clin. Epidemiol.* **61**, 344–349 (2008).
25. Nucci, M., Mapelli, D. & Mondini, S. Cognitive Reserve Index questionnaire (CRIq): a new instrument for measuring cognitive reserve. *Aging Clin. Exp. Res.* **24**, 218–226 (2012).
26. Della Rosa, P. A. et al. A Standardized [18F]-FDG-PET Template for Spatial Normalization in Statistical Parametric Mapping of Dementia. *Neuroinform* **12**, 575–593 (2014).
27. Brett, M., Anton, J. L., Valabregue, R. & Poline, J. B. Region of interest analysis using an SPM toolbox. *8th International Conference on Functional Mapping of the Human Brain. Neuroimage* **13**, 210–217 (2002).
28. Faillenot, I., Heckemann, R. A., Frot, M. & Hammers, A. Macroanatomy and 3D probabilistic atlas of the human insula. *NeuroImage* **150**, 88–98 (2017).
29. Lin, F. et al. Insula and Inferior Frontal Gyrus' Activities Protect Memory Performance Against Alzheimer's Disease Pathology in Old Age. *JAD* **55**, 669–678 (2016).
30. Park, D. C. & Reuter-Lorenz, P. The Adaptive Brain: Aging and Neurocognitive Scaffolding. *Annu. Rev. Psychol.* **60**, 173–196 (2009).
31. Bondi, M. W., Houston, W. S., Eyler, L. T. & Brown, G. G. fMRI evidence of compensatory mechanisms in older adults at genetic risk for Alzheimer disease. *Neurology* **64**, 501–508 (2005).
32. Uddin, L. Q., Nomi, J. S., Hébert-Seropian, B., Ghaziri, J. & Boucher, O. Structure and Function of the Human Insula. *J. Clin. Neurophysiol.* **34**, 300–306 (2017).
33. Simone, L. et al. Corrigendum to Anatomo-functional organization of insular networks: From sensory integration to behavioral control [Prog. Neurobiol. 247 (2025) 102748]. *Prog. Neurobiol.* **251**, 102795 (2025).
34. Menon, V. & Uddin, L. Q. Saliency, switching, attention and control: a network model of insula function. *Brain Struct. Funct.* **214**, 655–667 (2010).
35. Greicius, M. D., Krasnow, B., Reiss, A. L. & Menon, V. Functional connectivity in the resting brain: A network analysis of the default mode hypothesis. *Proc. Natl. Acad. Sci. U S A*. **100**, 253–258 (2003).
36. Liu, X. et al. Altered Functional Connectivity of Insular Subregions in Alzheimer's Disease. *Front. Aging Neurosci.* **10**, 107 (2018).

37. Agosta, F. et al. Resting state fMRI in Alzheimer's disease: beyond the default mode network. *Neurobiol. Aging*. **33**, 1564–1578 (2012).
38. Bialystok, E. & Bilingualism Pathway to Cognitive Reserve. *Trends Cogn. Sci.* **25**, 355–364 (2021).

Publisher's note Springer Nature remains neutral with regard to jurisdictional claims in published maps and institutional affiliations.

Authors and Affiliations

Rosa Liperoti[1,2] · Maria Camilla Cipriani[2] · Sonia Di Tella[3] · Isabella Anzuino[4] · Clio Scopetani Testa[4] · Eleonora Clemente[2] · Riccardo Calvani[1,2] · Maria Rita Lo Monaco[2] · Maria Lucia Calcagni[5,6] · Fabrizio Cocciolillo[6] · Maria Caterina Silveri[4]

✉ Maria Camilla Cipriani
mariacamilla.cipriani@policlinicogemelli.it

[1] Department of Geriatric and Orthopedic Sciences, Università Cattolica del Sacro Cuore, Rome, Italy

[2] Department of Geriatric, Orthopedic and Rheumatologic Sciences, Fondazione Policlinico Universitario A. Gemelli, IRCCS, Largo F. Vito 1, Rome 00168, Italy

[3] Experimental and Applied Psychology Laboratory, Department of Health and Life Sciences, Università Europea di Roma, Rome, Italy

[4] Department of Psychology, Università Cattolica del Sacro Cuore, Milan, Italy

[5] Department of Diagnostic Imaging, Oncological Radiotherapy and Hematology, Università Cattolica del Sacro Cuore, Rome, Italy

[6] Department of Diagnostic Imaging and Oncological Radiotherapy, Fondazione Policlinico Universitario A. Gemelli, IRCCS, Rome, Italy